

Degradation Kinetics of 2,4,6-Trinitrophenol from Water Using Atmospheric Air Cold Plasma

NGUYEN VAN HOANG* and NGUYEN CAO TUAN*^{ORCID}

Institute of New Technology, 17 Hoang Sam Street, Hanoi, Vietnam

*Corresponding authors: E-mail: minhtitvoi2009@gmail.com; tuansintep@gmail.com

Received: 29 November 2019;

Accepted: 29 January 2020;

Published online: 29 April 2020;

AJC-19844

The degradation studies of picric acid (2,4,6-trinitrophenol, TNP) in water sample through a dielectric barrier discharge (DBD) of atmospheric air cold plasma was carried out. The used DBD reactor consisted of comprised two electrodes that were separated by using an insulating dielectric barrier having a electric discharge voltage varying from of 7.0 to 22.0 kV. The effects of the initial concentration of TNP on the initial degradation rate was investigated methodically. The initial degradation rate was determined experimentally by changing the initial concentrations of TNP between 91.02 and 210.17 mg/L using the DBD of cold air plasma. From experimental results, a kinetic equation for TNP degradation was established based on varying initial concentration as $-R = 0.0252C_{\text{TNP}}/(1+0.0076C_{\text{TNP}})$. When $0.0076C_{\text{TNP}} \ll 1$, the kinetics of TNP degradation complied with the pseudo-first-order reaction. For TNP degradation kinetics, such as $\ln(C_t/C_0) = 0.0269t + 0.1605$, $\ln(C_t/C_0) = 0.0197t + 0.0792$, and $\ln(C_t/C_0) = 0.014t + 0.0623$, the initial concentrations of TNP were 91.02, 153.3 and 210.17 mg/L, respectively. Moreover, the effect of initial concentration of TNP and the electric power on the degradation efficiency of TNP were determined.

Keywords: 2,4,6-Trinitrophenol, Air cold plasma, Dielectric barrier discharge, Degradation, Kinetics.

INTRODUCTION

Matter exhibits four fundamental states *viz.* solid, liquid, gas and plasma, which depends on heat or energy addition [1]. Plasma, a characteristic fourth state of matter, is an ionized gas. According to the early studies, a plasma state can easily be attained in a gas-discharge tube, containing a gas with two-parallel metal electrodes. Under this condition, few inert gas molecules were ionized in the gas tube, which led to the formation of electron-ion pairs [2]. In an electric field, free electrons rapidly move toward an anode, causing the formation of a small background current of up to 10^{-6} ampere. When the voltage increases, primary electrons move further towards the anode, and from the applied electric field receive kinetic energy. The collision and subsequent reaction of primary electrons with inert gas atoms leads to the formation of secondary electron-ion pairs [3]. Plasma was employed as a dielectric barrier discharge (DBD) for developing industrial ozonators and DBD was used for environmental purposes and in industrial and medicinal applications [4]. The DBD reactor comprises two (planar) parallel electrodes, which are separated using a dielectric barrier. To

construct the dielectric barrier, one or both electrode/s can be coated with a dielectric material, such as quartz, silica, ceramic materials and mica. Quartz glass is most commonly used as the dielectric material [5].

Atmospheric pressure DBD current and a classical gas discharge exhibit similar characteristics. Because one electrode of DBD is coated and commenced by applying an AC-powered voltage to the anode (high-voltage electrode) [6]. Positive ions balance the electron density of plasma, making it electrically neutral [7,8]. Plasmas can produce a large number of chemically active and energetic species, such as ions, electrons, free radicals and atoms, which are in excited states. The $\cdot\text{OH}$ radicals and oxygen atoms produced during atmospheric air discharge play a crucial role in oxidation. Thus, plasma technology is widely used, especially, to treat wastewater containing recalcitrant organic compounds. Moreover, plasma is considered as a clean technology, which does not require additional chemicals [9,10]. Furthermore, cold plasma can be used to enhance dissolved oxygen amount, eliminate the odour from wastewater and reduce the chemical oxygen demand. However, cold plasma can lead to undesirable production of nitrite and nitrate. Cold plasma

treatment presents with other limitations of conductivity increase and pH reduction.

Due to environmental concerns, nitro-aromatic compounds present in wastewater must be eliminated through treatment before its discharge into rivers and/or oceans [11-14]. Apart from traditional treatments, for the degradation of nitro-aromatic compounds, such as 2,4,6-trinitrophenol (TNP), present in wastewater, advanced oxidation processes (AOPs) have received considerable attention [9,10]. Among AOPs, atmospheric air-cold plasma with reactive species, including $\cdot\text{OH}$, $\cdot\text{O}$, $\cdot\text{H}$, O_3 and H_2O_2 , has been obtained as most effective method for the degradation of nitro-aromatic compounds present in wastewater, and the wastewater obtained after treatment with plasma DBD was non-toxic [15-24]. The decomposition of TNP achieved using DBD is similar to that achieved using APOs, which is considerably complicated and proceeds through numerous intermediate stages. Thus, obtaining an accurate kinetic rate of TNP decomposition is difficult. In this study, several experiments were conducted to establish a kinetic equation for the decomposition rate of TNP, depending on its initial concentration. The decomposition reaction rate for the initial concentration of TNP did not depend on degradation intermediates obtained in the plasma reactor. Such a kinetic equation can be used in a treatment model on various scales.

EXPERIMENTAL

Analytical purity grade of solvents, chemicals and 2,4,6-trinitrophenol were obtained from Merck, U.S.A. and used without further purification. All the solutions were prepared prior to carrying out experiments and kept at room temperature. HPLC Model HP 1100 using diode-array detector Agilent (U.S.A.), Spectrophotometer UV-Vis Agilent 8453 (U.S.A.) and DR/890 Colorimeter, HACH was used for COD analysis.

Air cold plasma DBD reactor: The reactor comprises a high voltage pulse generator attached to an electrode system with water thin layer. A pump was employed to supply air (2-4 L/min) inside and outside the quartz tube of plasma chambers for enhancing ozone generation and ozone dissolution in water. A metering pump was utilized for circulating wastewater at a speed of 1.2 L/min in the reactor to increase the degradation efficiency of TNP.

Dielectric barrier discharge provides an electrical discharge between two electrodes separated through the insulating dielectric barrier [25,26]. Discharge was performed on a system of two coaxial electrodes that were separated using a thin insulating layer. In this study, a plasma DBD reactor comprising two electrodes, namely a grounded-central electrode (21 mm diameter) of inox steel and an outer copper electrode (HV) wrapped around the quartz tube (32 mm diameter) was used. The two coaxial electrodes were fixed on a Teflon insulated base. The plastic base was drilled for removing water from the plasma reactor. The voltage of insulating glass tubes was always high to obtain electrical sparks, which spread around the pipe evenly without pipe breakdown. A high voltage source (approximately > 10 kV) was connected the electrodes. DBD-cold plasma was obtained between a water layer and the inner surface of tube, because of sparks discharged in air between the outer surface of water layer and inside glass tube.

Atmospheric air cold plasma DBD treatment: A water sample was supplied to an inner electrode, which then flowed downward on the outer surface of a pipe wall and formed a 0.5 to 1 mm thin film (dependant of selected pump velocity). When the two electrodes were adjusted to obtain a sufficiently high voltage (approximately > 10 kV), DBD plasma was formed in the reactor chamber. Thus, DBD air-cold plasma with ozone, UV and other reactive reagents, such as $\cdot\text{H}$, $\cdot\text{OH}$, H_2O_2 was formed [13,27,28]. The aforementioned active components are considerably strong oxidizing agents for degrading pollutants present in wastewater. Fig. 1 presents the shapes of plasma DBD obtained from the atmospheric air-cold-plasma reactor.

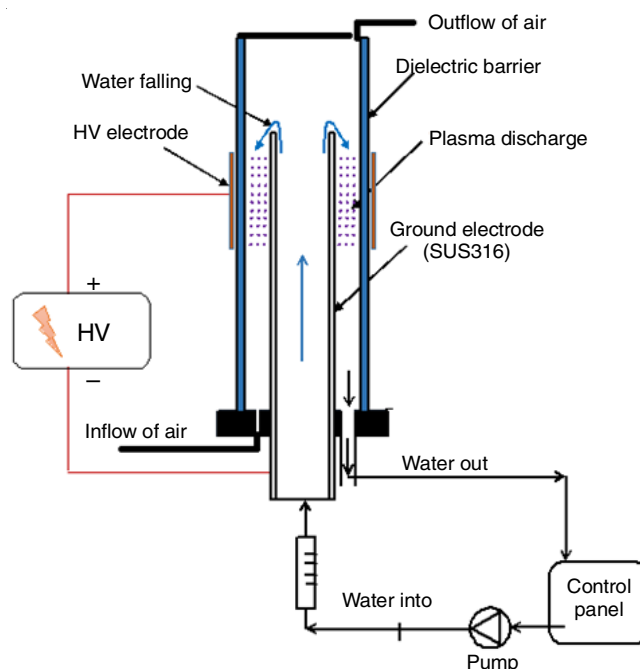


Fig. 1. Schematics of batch reactor configuration for plasma treatment

To enhance the efficiency of TNP decomposition, the wastewater samples were circulated. After an adequate time, the samples were removed from the reactor for HPLC analysis. In addition to analyze a decrease in the TNP concentration, external factors such as applied voltage and the effect of initial concentration of TNP on the decomposition efficiency were determined to establish kinetic equations for decomposition.

Determination of TNP concentration: A HPLC instrument was employed to determine the TNP concentration in the samples. The parameters of HPLC instrument comprised as: Detector: diode array; column of Hypersil C18 (200 × 4 mm); Mobile phase of acetonitrile/water: 65/35 (v/v); Pressure: 280 bar; pH = 7.

Procedure: A solution (5 μL) was taken from the reactor for HPLC analysis. Determine the retention time (t_R), peak height and peak area for calculating the TNP percentage remaining in the samples. The main parameters used for the HPLC analysis were measurement signal: 360 nm; flow rate: 0.35 mL/min; sample pump volume: 5.0 μL ; retention time (t_R): 4 min. A calibration curve was used to determine the TNP concentration.

Determination of COD index: The COD of sample was determined using the HACH COD DR/890 (USA) device accor-

ding to ISO 6060:1989: Water quality determination of COD. The determination was performed according to instructions provided with the device.

RESULTS AND DISCUSSION

Kinetics of degradation of 2,4,6-trinitrophenol

Degradation rate of TNP versus varying initial TNP concentration: Experimental conditions used for the analysis were as follows: applied power, voltage, wastewater circulation rate and sample pH were 16 mA, 19 kV, 415 mL/min, 3.2, respectively. The initial concentrations of TNP used were 91.02, 135.3 and 210.17 mg/L. A mean degradation rate of TNP was calculated after 30 min of treatment. Plasma DBD increased with an increase in the TNP concentration (Table-1).

Initial TNP concentration (mg/L)	0	91.02	135.3	210.17
TNP degradation rate (mg/L min)	0	1.35	1.71	2.01

Initially, the decomposition rate of TNP increased with an increase in the TNP concentration (Fig. 2). However, the mean rate of decomposition was not proportional to TNP concentrations. The mean rate of TNP degradation was measured after a 30 min of the reaction, which revealed an increase in the degradation rate of TNP with the increasing initial concentration of TNP. Under the experimental conditions, initial concentrations of TNP of < 210.17 mg/L provided an effective degradation.

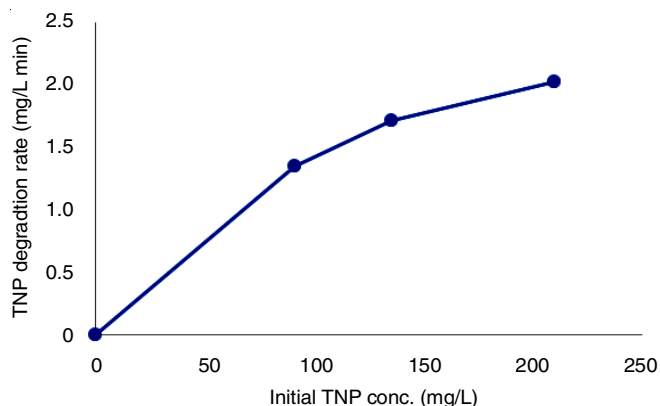


Fig. 2. TNP decomposition rate with initial TNP concentration (mg/L)

Fig. 3 indicates that the relationship between the reciprocal rate ($-1/R$) and reciprocal initial concentration of TNP ($1/C_{TNP}$) is a linear function of $-1/R = f(1/C_{TNP})$ of $y = 39.678x + 0.3009$

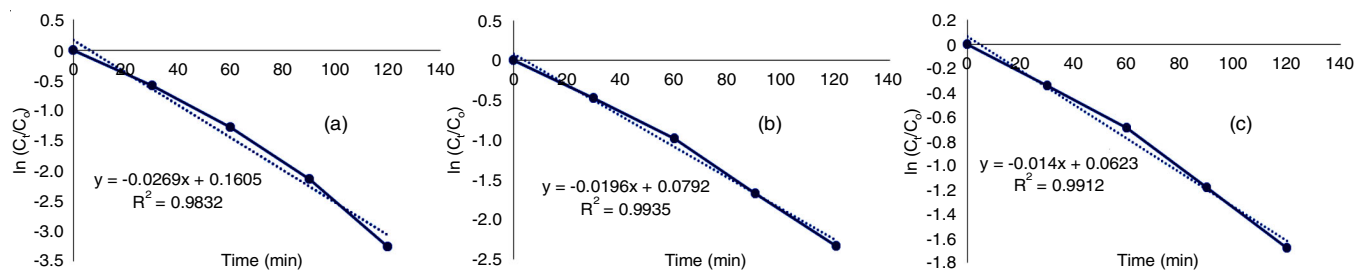


Fig. 4. Degradation kinetics of TNP at initial concentration of (a) 91.03 mg/L, (b) 135.3 mg/L and (c) 210.17 mg/L

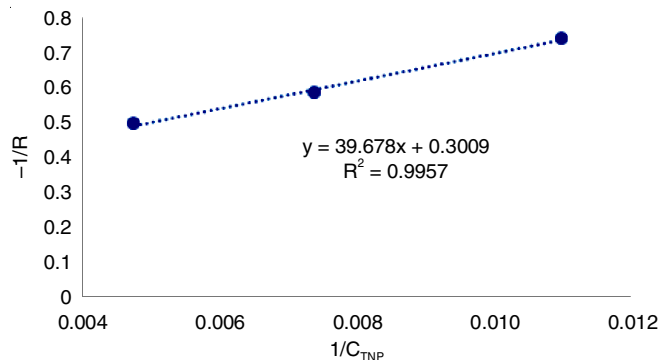


Fig. 3. Dependence curve of ($-1/R$) on ($1/C_{TNP}$)

and $R^2 = 0.9957$ or corresponding to the degradation rate of the empirical equation as follows:

$$-R = \frac{0.0252C_{TNP}}{1 + 0.0076C_{TNP}}$$

This expression is comparable to reported study [19], where the degradation kinetics of *p*-nitrophenol through Fenton reaction was studied.

When $0.0076C_{TNP} \ll 1$ or $C_{TNP} \ll 131.579$ mg/L, the degradation rate of TNP obtained after 30 min of reaction was proportional to the initial concentration, which was consistent with the experimental data (Fig. 3) from 0 to <135.3 mg/L.

Kinetics of TNP degradation in air cold plasma DBD reactor: The degradation kinetics of TNP were determined using three initial concentrations of TNP (91.02, 135.3 and 210.17 mg/L) and the reaction time varied from 30 to 120 min. The degradation kinetics of TNP in plasma DBD reactor obeyed the rate expression of pseudo-first-order reaction (Fig. 4).

From these equations, the half time of TNP degradation at different initial concentrations occurred in the plasma reactor were $t_{1/2}$ (91.03 mg/L) = 31.7 min; $t_{1/2}$ (153.3 mg/L) = 39.4 min and $t_{1/2}$ (210.17 mg/L) = 53.9 min.

By using the degradation rate equations of TNP, degradation reactions occurred in the plasma DBD reactor can be simplified, which obeyed the kinetics of the pseudo-first-order reaction.



$$-\frac{d(\text{TNP})}{dt} = k[\text{TNP}][\text{Reactive reagents}]$$

$$\text{or} \quad -\frac{d(\text{TNP})}{dt} = k_{\text{app}}[\text{TNP}]$$

where, $k_{\text{app}} = k[\text{reactive reagents}]$.

In this case, k_{app} depended on the ratio of reactive-reagent amount and initial concentrations of TNP. This conclusion is in accordance with the experimental results. The established kinetic equations of TNP degradation can be used to predict the TNP concentration remaining in plasma DBD reactors at any interval of treatment time.

Influence of applied power source on TNP degradation: For experiment, C_{TNP} and wastewater circulation rate were 135.3 mg/L and 415 mL/min, respectively with a varying-power source. The degradation efficiency (H%) of TNP was calculated based on the following expression:

$$H(\%) = \frac{C_{TNP_0} - C_{TNP_t}}{C_{TNP_0}} \times 100$$

The experimental data (Table-2) indicated that with an increase in the applied power from 16 to 21 kV, the TNP degradation rate and degradation efficiency increased (Fig. 5), since more reactive species were produced at a higher voltage leading to an increase in degradation.

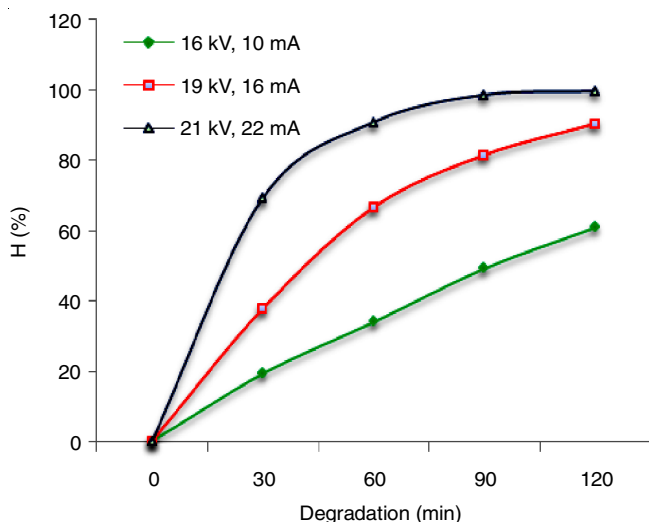


Fig. 5. Degradation efficiency (H%) of TNP with varying power sources

Mineralization of TNP: The mineralization of TNP was determined according to the decrease in COD values and TNP concentration obtained after treatment in the plasma DBD reactor at a voltage of 19 kV and I of 16 mA. The experimental results (Fig. 6) indicated that after 240 min of treatment, TNP present in the samples was nearly completely degraded, whereas 134 mg of O_2 , corresponding to 57% COD treated. This finding indicated that the TNP degradation occurred in several steps and in the first step, TNP was transformed into other compounds.

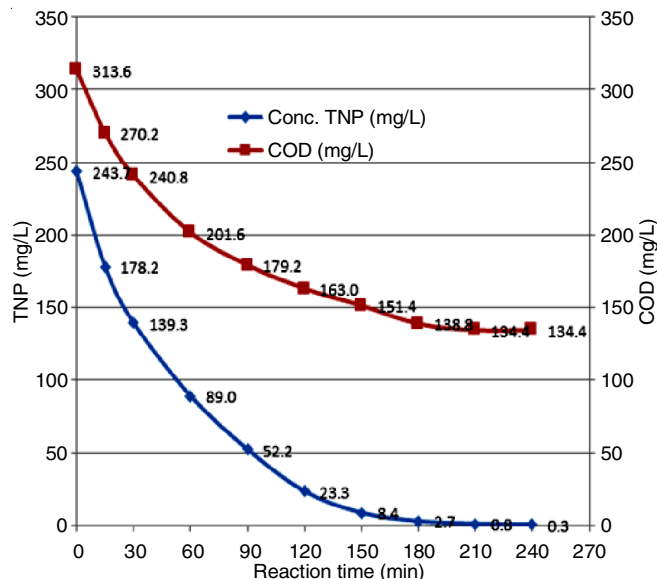


Fig. 6. Response of TNP concentration and COD values with time

Conclusion

In this study, atmospheric air-cold plasma with dielectric barrier reactor was developed to investigate the degradation of picric acid (2,4,6-trinitrophenol, TNP) in water. The plasma reactor comprises a power source varying in a range of 16-21 kV with two coaxial electrodes separated using Quartz glass-dielectric barrier. The effect of initial concentrations of TNP ranged between 91.02 and 210.17 mg/L on the degradation efficiency and the reaction time was investigated to determine the kinetics of TNP degradation. Under experimental conditions, TNP degradation obeyed the rate kinetics of the pseudo-first-order reaction. A decrease in the COD values and TNP concentration revealed that TNP degradation occurred in plasma DBD reactor proceeds through several steps, and the first step may be the transformation of TNP into other intermediate compounds.

ACKNOWLEDGEMENTS

The authors gratefully acknowledge Prof. Dang Kim Chi, Hanoi University of Science and Technology, Prof. Kun-Yi Andrew Lin, National Chung Hsing University and Tran Van Chung, Institute of Chemistry and Materials, Hanoi, Vietnam for their assistance with particular technique and methodology.

CONFLICT OF INTEREST

The authors declare that there is no conflict of interests regarding the publication of this article.

TABLE-2
INFLUENCE OF POWER SOURCE ON TNP DEGRADATION, $C_{TNP} = 135.30$ mg/L

Time (min)	I = 10 mA, U = 16 kV			I = 16 mA, U = 19 kV			I = 22 mA, U = 21 kV		
	C_t (mg/L)	H (%)	R (mg/L min)	C_t (mg/L)	H (%)	R (mg/L min)	C_t (mg/L)	H (%)	R (mg/L min)
0	135.30	–	–	135.30	–	–	135.30	–	–
30	109.01	19.43	0.88	84.20	37.77	1.70	41.86	69.21	3.11
60	89.20	34.07	0.66	50.19	62.90	1.13	11.65	91.54	1.01
90	68.59	49.31	0.69	25.08	81.47	0.84	2.11	98.59	0.32
120	52.82	60.96	0.53	13.05	90.36	0.40	0.70	99.63	0.05

REFERENCES

1. T. Yamamoto and M. Okubo, eds.: L.K. Wang, Y.-T. Hung and N.K. Shammass, *Nonthermal Plasma Technology*, In: *Handbook of Environmental Engineering, Advanced Physicochemical Treatment Technologies*, Humana Press: New York, vol. 5, pp. 135-293 (2007).
2. H. Conrads and M. Schmidt, *Plasma Sources Sci. Technol.*, **9**, 441 (2000); <https://doi.org/10.1088/0963-0252/9/4/301>
3. Y. Raizer, *Gas Discharge Physics*, Springer-Verlag, Berlin: pp 449 (1987).
4. B. Eliasson, M. Hirth and U. Kogelschatz, *J. Phys. D Appl. Phys.*, **20**, 1421 (1987); <https://doi.org/10.1088/0022-3727/20/11/010>
5. H.-E. Wagner, R. Brandenburg, K.V. Kozlov, A. Sonnenfeld, P. Michel and J.F. Behnke, *Vacuum*, **71**, 417 (2003); [https://doi.org/10.1016/S0042-207X\(02\)00765-0](https://doi.org/10.1016/S0042-207X(02)00765-0)
6. U. Kogelschatz, *Plasma Chem. Plasma Process.*, **23**, 1 (2003); <https://doi.org/10.1023/A:1022470901385>
7. M. López, T. Calvo, M. Prieto, R. Múgica-Vidal, I. Muro-Fraguas, F. Alba-Elías and A. Alvarez-Ordóñez, *Front. Microbiol.*, **10**, 622 (2019); <https://doi.org/10.3389/fmicb.2019.00622>
8. Y.-M. Zhao, M. de Alba, D.-W. Sun and B. Tiwari, *J. Critical Rev. Food Sci. Nutr.*, **59**, 728 (2019); <https://doi.org/10.1080/10408398.2018.1495613>
9. C. Hoffmann, C. Berganza and J. Zhang, *Med. Gas Res.*, **3**, 21 (2013); <https://doi.org/10.1186/2045-9912-3-21>
10. Z. Chen, X. Cheng, L. Lin and M. Keidar, *J. Phys. D: Appl. Phys.*, **50**, 015208 (2017); <https://doi.org/10.1088/1361-6463/50/1/015208>
11. C.M. Peres and S.N. Agathos, *Biotechnol. Ann. Rev.*, **6**, 197 (2000); [https://doi.org/10.1016/S1387-2656\(00\)06023-3](https://doi.org/10.1016/S1387-2656(00)06023-3)
12. F.D. Marvin-Sikkema and J.A.M. de Bont, *Appl. Microbiol. Biotechnol.*, **42**, 499 (1994); <https://doi.org/10.1007/BF00173912>
13. M.-W. Chang, T.-S. Chen and J.-M. Chern, *Ind. Eng. Chem. Res.*, **47**, 8533 (2008); <https://doi.org/10.1021/ie8003013>
14. J.L. Wang and L.J. Xu, *J. Crit. Rev. Environ. Sci. Technol.*, **42**, 251 (2012); <https://doi.org/10.1080/10643389.2010.507698>
15. J. Bergendahl and J. O'Shaughnessy, *J. New England Water Environ. Assoc.*, **38**, 1979 (2004).
16. P.M.K. Reddy and C. Subrahmanyam, *Ind. Eng. Chem. Res.*, **51**, 11097 (2012); <https://doi.org/10.1021/ie301122p>
17. E. Marotta, M. Schiorlin, X. Ren, M. Rea and P. Paradisi, *Plasma Process. Polym.*, **8**, 867 (2011); <https://doi.org/10.1002/ppap.201100036>
18. M. Magureanu, D. Piroi, N.B. Mandache and V. Parvulescu, *J. Appl. Phys.*, **104**, 103306 (2008); <https://doi.org/10.1063/1.3021452>
19. H.-H. Cheng, S.-S. Chen, Y.-C. Wu and D.-L. Ho, *J. Environ. Eng. Manage.*, **17**, 427 (2007).
20. N. Van Hoang, N.C. Tuan and D.K. Chi, *Int. J. Develop. Res.*, **8**, 23260 (2018).
21. A. Fridman, *Plasma Chemistry*, Cambridge University Press: New York (2008).
22. E.S. Massima Mouele, O.O. Fatoba, O. Babajide, K.O. Badmus and L.F. Petrik, *Environ. Sci. Pollut. Res. Int.*, **25**, 9265 (2018); <https://doi.org/10.1007/s11356-018-1392-9>
23. P.J. Bruggeman, M.J. Kushner, B.R. Locke, J.G.E. Gardeniers, W.G. Graham, D.B. Graves, R.C.H.M. Hofman-Caris, D. Maric, J.P. Reid, E. Ceriani, D. Fernandez Rivas, J.E. Foster, S.C. Garrick, Y. Gorbanev, S. Hamaguchi, F. Iza, H. Jablonowski, E. Klimova, J. Kolb, F. Krcma, P. Lukes, Z. Machala, I. Marinov, D. Mariotti, S. Mededovic Thagard, D. Minakata, E.C. Neyts, J. Pawlat, Z.L. Petrovic, R. Pflieger, S. Reuter, D.C. Schram, S. Schröter, M. Shiraiwa, B. Tarabová, P.A. Tsai, J.R.R. Verlet, T. von Woedtke, K.R. Wilson, K. Yasui and G. Zvereva, *Plasma Sources Sci. Technol.*, **25**, 053002 (2016); <https://doi.org/10.1088/0963-0252/25/5/053002>
24. C. Cathey, J. Cain, H. Wang, M.A. Gundersen, C. Carter and M. Ryan, *Combust. Flame*, **154**, 715 (2008); <https://doi.org/10.1016/j.combustflame.2008.03.025>
25. I. Hamouda, J. Guillem-Martí, M.P. Ginebra and C. Canal-Barnilís, *Biomecánica*, **25**, 1(8) (2017); <https://doi.org/10.5821/sibb.25.1.5384>
26. H. Mahvi, E. Bazrafshan, Gh.R. Jahed, *Pak. J. Biol. Sci.*, **8**, 892 (2005); <https://doi.org/10.3923/pjbs.2005.892.894>
27. M. Restiwijaya, A.R. Hendrini, B. Dayana, E. Yulianto, A.W. Kinandana, F. Arianto, E. Sasmita, M. Azam and M. Nur, *J. Phys. Conf. Ser.*, **1170**, 012020 (2019); <https://doi.org/10.1088/1742-6596/1170/1/012020>
28. V.E. Malanichev, M.V. Malashin, S.I. Moshkunov and V.Yu. Khomich, *High Energy Chem.*, **50**, 304 (2016); <https://doi.org/10.1134/S0018143916040111>